

# Synthesis, spectral characterization, electrochemical studies and catalytic properties in Suzuki–Miyaura coupling reactions of the mononuclear $\text{Pd}^{\text{II}}$ , trinuclear $\text{Pd}^{\text{II}}(\text{BPh}_2)_2$ and $\text{Ru}^{\text{II}}-\text{Pd}^{\text{II}}-\text{Ru}^{\text{II}}$ type complexes containing 4-amino-1-benzyl piperidine and phenyl groups

Ahmet Kilic<sup>a\*</sup>, Ismail Yilmaz<sup>b</sup>, Mahmut Ulusoy<sup>c</sup> and Esref Tas<sup>a</sup>

The ligand containing the 4-amino-1-benzyl piperidine group, *N,N'*-(4-amino-1-benzyl piperidine)-glyoxime, ( $\text{LH}_2$ ) (1) was prepared from 4-amino-1-benzyl piperidine with *anti*-dichloroglyoxime at  $-15^\circ\text{C}$  in absolute Tetrahydrofuran (THF). In the trinuclear  $[\text{Pd}(\text{L})_2\text{Ru}_2(\text{phen})_4](\text{ClO}_4)_2$  (4) and  $[\text{Pd}(\text{L})_2\text{Ru}_2(\text{bpy})_4](\text{ClO}_4)_2$  (5) metal complexes, the  $\text{Pd}^{\text{II}}$  ion centered into the main oxime core by the coordination of the imino groups while the two  $\text{Ru}^{\text{II}}$  ions coordinated dianionic oxygen donors of the oxime groups and linked to the ligands of 1,10-phenanthroline and 2,2'-bipyridine. The mono and trinuclear metal complexes were characterized by elemental analyses, FT-IR, UV–vis,  $^1\text{H}$  and  $^{13}\text{C}$ -NMR spectra, magnetic susceptibility measurements, molar conductivity, cyclic voltammetry, mass spectra, X-ray powder techniques and their morphology by SEM measurements. The cyclic voltammetric results show that the cathodic peak ( $E_{\text{pc}}$ ) potential of (3) shifts towards more positive values compared with that of (2) as a result of the  $\text{BPh}_2^+$ -bridged complex formation. The Suzuki–Miyaura reaction was used to investigate their activity as catalyst either prepared *in-situ* or from well-defined complexes. Copyright © 2008 John Wiley & Sons, Ltd.

**Keywords:** Ru(II) metal complexes; synthesis; spectroscopy; electrochemistry; catalytic activity; cross-coupling; Suzuki–Miyaura reactions

## Introduction

The study of the coordination of transition metal ions to different types of ligand has been encouraged by the recent developments in the fields of bioinorganic chemistry and medicine. Knowledge of coordination chemistry is essential to the understanding of the structural and functional features of metalloproteins, and medical applications range from the development of MRI contrasting agents, radiopharmaceuticals and chemotherapeutics to the treatment of metal toxicity.<sup>[1]</sup> The synthesis of *vic*-dioximes and their different derivatives has been the subject of study for very a long period of time. The transition metal complexes of *vic*-dioximes have been of particular interest as biological model compounds.<sup>[2]</sup> Moreover, *vic*-dioximes are interesting for many applications in a variety of high technology fields, such as medicine,<sup>[3–5]</sup> catalysis,<sup>[6,7]</sup> electro-optical sensors,<sup>[8]</sup> liquid crystals<sup>[9]</sup> and trace metal analysis.<sup>[10]</sup> Pd- and Ni-catalyzed Suzuki–Miyaura cross-coupling is the most important and efficient strategy for the construction of unsymmetrical biaryl compounds and has attracted much current interest.<sup>[11]</sup> This cross-coupling methodology allows the use of organic solvents and inorganic bases, tolerates many functional groups, is not affected by steric hindrance of the substrates, and is suitable for industrial processes.<sup>[12]</sup> Trinuclear (4 and 5)

type complexes having a ligand with nitrogen and oxygen donor atoms show DNA binding and antitumor activity.<sup>[13]</sup> The possibility of an apical modification of *vic*-dioximes is stipulated by the relative availability of functionalized boron-containing Lewis acids as efficient capping agents. Borylation significantly alters the character of the glyoxime complexes; solubility, color, reactivity, etc.<sup>[14]</sup> The nature of the ligands around the metal has been found to dramatically affect the energy conversion process. In particular, the introduction of electronic effects via electron-donor substituents on 2,2'-bipyridine (bpy) and 1,10-phenanthroline (phen) ligands notably improved the absorption in the visible region for efficient sunlight collection.<sup>[15]</sup> These complexes have enabled us to systematically probe the phenomenon of proton-coupled electron transfer that occurs when oxime ligand is

\* Correspondence to: Ahmet Kilic, Department of Chemistry, University of Harran, 63190, Sanliurfa, Turkey. E-mail: Kilica63@harran.edu.tr

a Department of Chemistry, University of Harran, 63190, Sanliurfa, Turkey

b Department of Chemistry, Technical University of Istanbul, 34469, Istanbul, Turkey

c Department of Chemistry, University of Ege, 35100, Izmir, Turkey

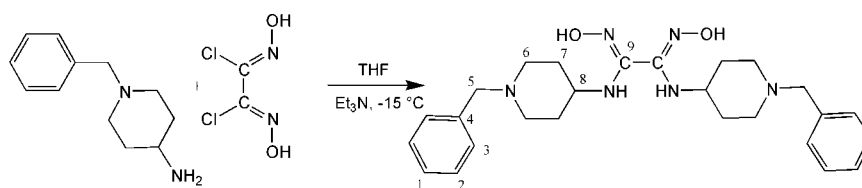


Figure 1. Synthesis of ligand (LH<sub>2</sub>).

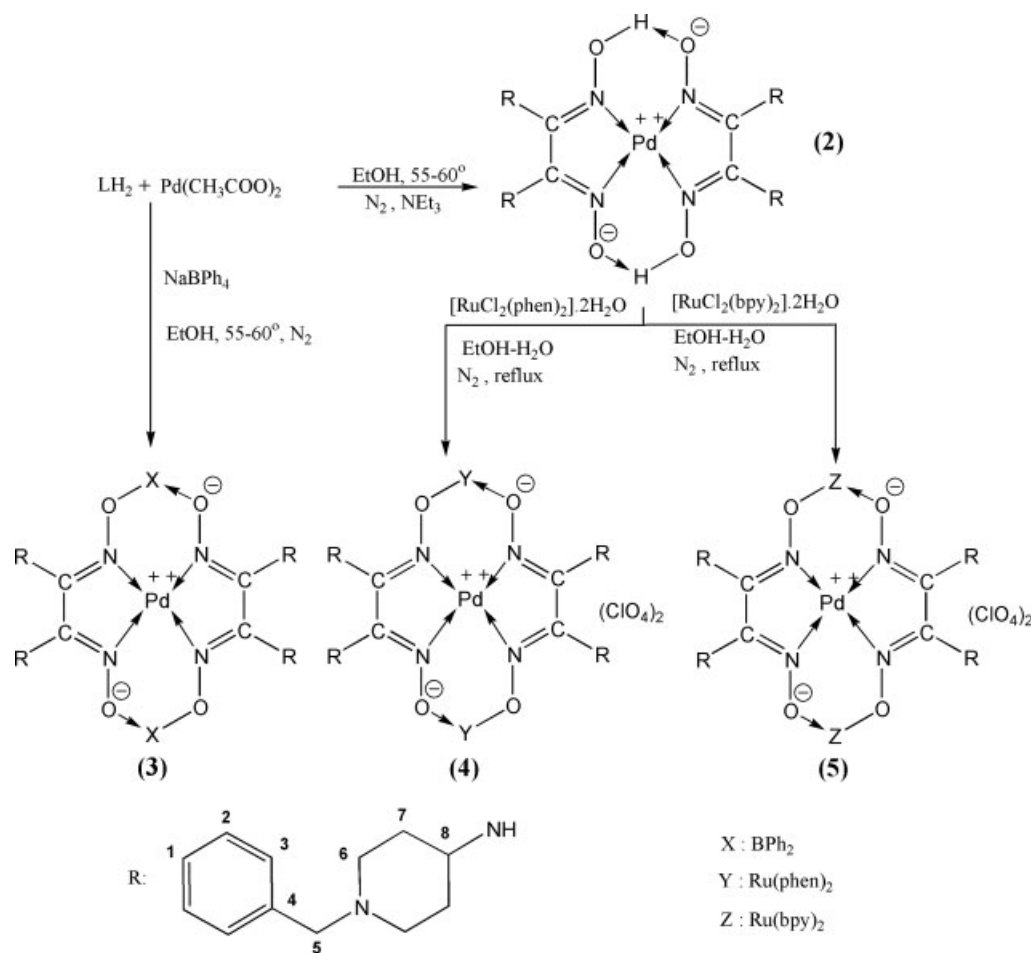


Figure 2. The proposed structure for the metal complexes.

coordinated to a redox active metal center. Herein, we have prepared ligand with mononuclear (2) and trinuclear (3–5) compounds as shown in Figs 1 and 2. Synthesis, characterization, spectroscopic, electrochemical catalytic properties as catalysts in Suzuki–Miyaura coupling reactions of the new *vic*-dioxime metal complexes have been investigated in detail. The ligand and its metal complexes have been identified by a combination of elemental analyses, <sup>1</sup>H-NMR and <sup>13</sup>C-NMR spectra, FT-IR spectra, UV–vis spectra, magnetic susceptibility measurements, mass spectra, X-ray powder diffraction measurements, molar conductivity measurements, cyclic voltammetric techniques and their morphology by SEM measurements. The first aim of this study was to prepare a new highly soluble trinuclear *vic*-dioxime complex (3–5) metal complexes. The second aim was to compare their electrochemical behavior to understand the effect of the coordination of the BPh<sub>2</sub><sup>+</sup>-capped ion or bidentate ligands such as 1,10-phenanthroline and 2,2′-bipyridine to the oxime moieties

through two oxygen donor atoms. The third aim was to understand their crystalline or amorphous structures by X-ray powder analysis as well. The fourth aim was to find a suitable, influential and easily prepared catalyst valid in a wide range of C–C bond forming processes.

## Experimental

All reagents and solvents were of reagent-grade quality and obtained from commercial suppliers (Fluka Chemical Company, Taufkirchen, Germany). Tetra-*n*-butylammonium perchlorate (TBAP, Fluka) was used as received. [RuCl<sub>2</sub>(phen)<sub>2</sub>].2H<sub>2</sub>O and [RuCl<sub>2</sub>(bpy)<sub>2</sub>].2H<sub>2</sub>O were prepared by a literature method.<sup>[16]</sup> The C, H, N elemental analyses were performed on a LECO CHNS-932 model analyzer. The elemental analyses were carried out in the Laboratory of the Scientific and Technical Research Center of Inonu University. IR spectra were recorded on a Perkin Elmer Spectrum

RX FT-IR Spectrometer as KBr pellets.  $^1\text{H}$ -NMR and  $^{13}\text{C}$ -NMR spectra were recorded on a Bruker-Avance 400 MHz spectrometers. Magnetic susceptibilities were determined on a Sherwood Scientific Magnetic Susceptibility Balance (Model MK1) at room temperature (20 °C) using  $\text{Hg}[\text{Co}(\text{SCN})_4]$  as a calibrant; diamagnetic corrections were calculated from Pascal's constants.<sup>[17]</sup> UV-vis spectra were recorded on a Perkin Elmer Lambda 25 PC UV-vis spectrometer. Molar conductivities ( $\Lambda_{\text{M}}$ ) were recorded on a Inolab Terminal 740 WTW Series. MS results were recorded on a Micromass Quatro LC/ULTIMA LC-MS/MS spectrometer. X-ray powder were recorded on a Rigaku Ultima III Series. The scanning electron microscopy (SEM) measurements were carried out on a Zeiss Evo 50 Series. The samples were sputter coated with carbon by Balzers Med 010 to prevent charging when analyzed by the electron beam. Cyclic voltammograms (CV) were carried out using CV measurements with Princeton Applied Research Model 2263 potentiostat controlled by an external PC. A three-electrode system (BAS model solid cell stand) was used for CV measurements in DMSO and consisted of a 2 mm sized platinum disk electrode as working electrode, a platinum wire counter electrode, and an Ag-AgCl reference electrode. The reference electrode was separated from the bulk solution by a fritted-glass bridge filled with the solvent/supporting electrolyte mixture. The ferrocene-ferrocenium couple ( $\text{Fc}-\text{Fc}^+$ ) was used as an internal standard but all potentials in the paper are referenced to the Ag-AgCl reference electrode. Solutions containing complexes were deoxygenated by a stream of high-purity nitrogen for at least 5 min. Before running the experiment and during the experiment, the solution was protected from air by a blanket of nitrogen. Controlled potential electrolysis (CPE) was performed with Princeton Applied Research Model 2263 potentiostat/galvanostat. An BAS model electrolysis cell with a fritted glass to separate the cathodic and anodic portions of the cell was used for bulk electrolysis. The sample and solvent were placed into the electrolysis cell under nitrogen.

### Synthesis of the ligand ( $\text{LH}_2$ ) (1)

The synthesis of the ligand ( $\text{LH}_2$ ) has been reported previously.<sup>[18]</sup> Ligand ( $\text{LH}_2$ ) is soluble in common organic solvents such as THF, EtOH, DMF and DMSO. Yield: (84%), Color: yellow, m.p. = 143 °C. Anal. calcd for  $\text{C}_{26}\text{H}_{35}\text{N}_6\text{O}_2$  (MW: 465 g/mol): C, 67.24; H, 7.76; N, 18.10. Found: C, 67.21; H, 7.62; N, 17.98. IR (KBr pellets,  $\nu_{\text{max}}/\text{cm}^{-1}$ ): 3617–3143  $\nu(\text{OH}/\text{NH})$ , 3028  $\nu(\text{Ar}-\text{H})$ , 2941, 2765  $\nu(\text{Aliph}-\text{H})$ , 1638  $\nu(\text{C}=\text{N})$ , 1367 and 983  $\nu(\text{N}-\text{O})$ . UV-vis ( $\lambda_{\text{max}}$ , nm): 230, 242 (in  $\text{CH}_2\text{Cl}_2$ ) and 268, 353 (in DMSO). MS (LSI, Scan  $\text{ES}^+$ ): ( $m/z$ ) 465 [ $\text{M}]^+$ ,  $^1\text{H}$ -NMR ( $\text{CDCl}_3$ , TMS,  $\delta$  ppm): 9.56 (s, 2H, OH), 7.31–7.26 (m, 10H, Ar-CH), 5.15–5.13 (d, 2H,  $J = 9.6$ , NH), 3.50 (s, 4H,  $\text{N}-^5\text{CH}_2$ ), 2.82–2.80 (d, 2H,  $J = 8$ , N-CH), 2.07–2.01 (m, 8H,  $\text{N}-^6\text{CH}_2$ ), 1.85–1.83 (d, 4H,  $J = 8$ , Cyc-CH<sub>2</sub>) and 1.60–1.55 (m, 4H, Cyc-CH<sub>2</sub>).  $^{13}\text{C}$ -NMR ( $\text{CDCl}_3$ , TMS,  $\delta$  ppm):  $\text{C}_1$ (127.25),  $\text{C}_2$ (128.27),  $\text{C}_3$ (129.57),  $\text{C}_4$ (137.42),  $\text{C}_5$ (62.97),  $\text{C}_6$ (52.23),  $\text{C}_7$ (34.70),  $\text{C}_8$ (49.99) and  $\text{C}_9$ (147.65).

### Synthesis of the $[\text{Pd}(\text{LH}_2)_2]$ metal complex (2)

A solution of palladium(II) acetate (0.24 g, 1.07 mmol) in absolute ethanol (30  $\text{cm}^3$ ) was added to a solution of ligand ( $\text{LH}_2$ ) (1.0 g, 2.14 mmol), in absolute ethanol (70  $\text{cm}^3$ ) at 55–60 °C. A distinct change was observed in color from colorless to orange under an  $\text{N}_2$  atmosphere with continuous stirring. Then, a decrease in the pH of the solution was observed. The pH of the solution was ca. 1.5–3.0 and was adjusted to 4.5–5.5 by the addition of

a 1% triethylamine solution in EtOH. After heating the mixture for 6 h in a water bath, the precipitate was filtered off, washed with  $\text{H}_2\text{O}$  and diethyl ether several times, and dried *in vacuo* at 35 °C. Yield: (66%), Color: brown, m.p. = 190 °C. Anal. calcd for  $\text{C}_{52}\text{H}_{70}\text{N}_{12}\text{O}_4\text{Pd}$  (MW: 1032 g/mol): C, 60.47; H, 6.78; N, 16.28. Found: C, 60.36; H, 6.65; N, 16.39.  $\Lambda_{\text{M}} = 10/\Omega/\text{cm}^2/\text{mol}$ , IR (KBr pellets,  $\nu_{\text{max}}/\text{cm}^{-1}$ ): 3564–3132  $\nu(\text{O}-\text{H} \cdots \text{O}/-\text{NH})$ , 3027  $\nu(\text{Ar}-\text{H})$ , 2937, 2758  $\nu(\text{Aliph}-\text{H})$ , 1726  $\nu(\text{O}-\text{H} \cdots \text{O})$ , 1610  $\nu(\text{C}=\text{N})$ , 1338  $\nu(\text{N}-\text{O})$ . UV-vis ( $\lambda_{\text{max}}$ , nm): 238, 298, 437 (in  $\text{CH}_2\text{Cl}_2$ ) and 256, 260, 300, 441 (in DMSO). MS (LSI, Scan  $\text{ES}^+$ ): ( $m/z$ ) 1031 [ $\text{M}]^+$ ,  $^1\text{H}$ -NMR ( $\text{DMSO}-d_6$ , TMS,  $\delta$  ppm): 16.24 (s, 2H, O-H  $\cdots$  O), 7.33–7.21 (m, 20H, Ar-CH), 5.82 (s, 4H, NH), 3.42–3.40 (d, 8H,  $J = 7.2$ ,  $\text{N}-^5\text{CH}_2$ ), 2.75–2.65 (m, 4H, N-CH), 2.30–2.38 (m, 16H,  $\text{N}-^6\text{CH}_2$ ), 1.95–1.74 (m, 8H, Cyc-CH<sub>2</sub>) and 1.43–1.40 (m, 8H, Cyc-CH<sub>2</sub>).  $^{13}\text{C}$ -NMR ( $\text{DMSO}-d_6$ , TMS,  $\delta$  ppm):  $\text{C}_1$ (127.56),  $\text{C}_2$ (128.68),  $\text{C}_3$ (129.43),  $\text{C}_4$ (139.01),  $\text{C}_5$ (62.15),  $\text{C}_6$ (52.95),  $\text{C}_7$ (33.23),  $\text{C}_8$ (51.83) and  $\text{C}_9$ (152.16).

### Synthesis of the $[\text{Pd}(\text{L}_2)(\text{BPh}_2)_2]$ metal complex (3)

To a solution of ligand ( $\text{LH}_2$ ) (0.54 g, 1.08 mmol) in 120 ml of warm absolute ethanol (55–60 °C) was added a solution of palladium(II) acetate (0.12 g, 0.54 mmol) in 30 ml of warm absolute ethanol (55–60 °C) with stirring. The color of the solution turned to red and then the ethanol solution was cooled to room temperature. A solution of excess  $\text{NaBPh}_4$  in 40 ml absolute ethanol was added dropwise to this clear red solution. A distinct change was observed in color from red to orange under a  $\text{N}_2$  atmosphere with continuous stirring. Then the ethanol removed under reduced pressure. The orange solid compound was dissolved with  $\text{CH}_2\text{Cl}_2$  (90 ml). The solution was filtered, extracted with water and then filtered. Removal of  $\text{CH}_2\text{Cl}_2$  gave an orange solid which was recrystallized from  $\text{CH}_2\text{Cl}_2/\text{EtOH}$  (1 : 8) to give orange crystals which were filtered, washed with EtOH, diethylether and dried. Yield, 64%; color, dark yellow; m.p. = 129 °C. Anal. calcd for  $\text{C}_{76}\text{H}_{88}\text{N}_{12}\text{O}_4\text{B}_2\text{Pd}$  (MW: 1361 g/mol) : C, 67.00; H, 6.47; N, 12.34. Found: C, 67.08; H, 6.38; N, 12.27,  $\Lambda_{\text{M}} = 30/\Omega/\text{cm}^2/\text{mol}$ ,  $\mu_{\text{eff}} = \text{Dia}$ , IR (KBr pellets,  $\nu_{\text{max}}/\text{cm}^{-1}$ ): 3354  $\nu(\text{NH})$ , 3061  $\nu(\text{Ar}-\text{H})$ , 2928–2764  $\nu(\text{Aliph}-\text{H})$ , 1600  $\nu(\text{C}=\text{N})$ , 1199  $\nu(\text{B}-\text{O})$ , 878  $\nu(\text{B}-\text{Ph})$ , 1367  $\nu(\text{N}-\text{O})$ , 741 and 702  $\nu(\text{Ar}-\text{H})$ . UV-vis ( $\lambda_{\text{max}}$ , nm): 234, 244, 248, 310 (in  $\text{CH}_2\text{Cl}_2$ ) and 262, 322, 403 (in DMSO), MS (LSI, Scan  $\text{ES}^+$ ): ( $m/z$ ) 1360 [ $\text{M}]^+$ ,  $^1\text{H}$ -NMR ( $\text{DMSO}-d_6$ , TMS,  $\delta$  ppm): 7.77–7.75 (t, 4H,  $J = 7.6$ , Ar-CH), 7.65–7.63 (t, 4H,  $J = 8.4$ , Ar-CH), 7.46–7.11 (m, 16H, Ar-CH), 7.03–6.72 (m, 16H, Ar-CH), 5.68–5.65 (d, 4H,  $J = 12$ , NH), 3.58 (s, 8H,  $\text{N}-^5\text{CH}_2$ ), 2.67–2.64 (t, 4H,  $J = 12$ , N-CH), 2.35–2.31 (t, 16H,  $J = 16$ ,  $\text{N}-^6\text{CH}_2$ ), 1.96–1.94 (m, 8H, Cyc-CH<sub>2</sub>) and 1.26 (s, 8H, Cyc-CH<sub>2</sub>).  $^{13}\text{C}$ -NMR ( $\text{DMSO}-d_6$ , TMS,  $\delta$  ppm):  $\text{C}_1$ (127.26),  $\text{C}_2$ (128.42),  $\text{C}_3$ (128.91),  $\text{C}_4$ (138.03),  $\text{C}_5$ (63.10),  $\text{C}_6$ (53.31),  $\text{C}_7$ (33.97),  $\text{C}_8$ (51.95),  $\text{C}_9$ (149.62),  $\text{C}_{10}$ (132.16),  $\text{C}_{11}$ (127.68),  $\text{C}_{12}$ (127.46) and  $\text{C}_{13}$ (126.14).

### Synthesis of the $[\text{Pd}(\text{L}_2)\text{Ru}_2(\text{X})_4]$ metal complexes (4 and 5)

The complexes  $[\text{Pd}(\text{L}_2)\text{Ru}_2(\text{phen})_4](\text{ClO}_4)_2$  (**4**) and  $[\text{Pd}(\text{L}_2)\text{Ru}_2(\text{bpy})_4](\text{ClO}_4)_2$  (**5**) (where X = phen = 1,10 phenanthroline and bpy = 2,2'-bipyridine) were synthesized using a method similar to that described in Llanguri *et al.*<sup>[17]</sup>  $[\text{RuCl}_2(\text{phen})_2] \cdot 2\text{H}_2\text{O}$  (0.1 g, 0.17 mmol) and  $[\text{RuCl}_2(\text{bpy})_2] \cdot 2\text{H}_2\text{O}$  (0.1 g, 0.19 mmol) were refluxed in an ethanol–water mixture (40 : 10ml) for 55 min. The complex **2** (0.35 g, 0.34 mmol for **4** and 0.39 g, 0.38 mmol for **5**) was then added and heating was maintained for 20–22 h. The resulting dark-red solutions were cooled to room temperature. Next, the solvent was removed from the solutions obtained under vacuum

and with smooth heating. The crude products were dissolved in 25 ml of distilled water and the final products were precipitated after adding NaClO<sub>4</sub> solutions. Then, the final products were washed three times in water (15 ml) and diethyl ether (15 ml). The products were recrystallized from a mixture of CHCl<sub>3</sub>–EtOH.

#### [Pd(L)<sub>2</sub>Ru<sub>2</sub>(phen)<sub>4</sub>](ClO<sub>4</sub>)<sub>2</sub> (**4**)

Yield, 60%; color, dark brown; m.p. = 201 °C.  $\Delta_M = 208/\Omega/\text{cm}^2/\text{mol}$ ,  $\mu_{\text{eff}} = \text{Dia}$ ; IR (KBr pellets,  $\nu_{\text{max}}/\text{cm}^{-1}$ ): 3362  $\nu(\text{NH})$ , 3060  $\nu(\text{Ar-H})$ , 2954–2853  $\nu(\text{Aliph-H})$ , 1603  $\nu(\text{C=N})$ , 1378  $\nu(\text{N-O})$ , 1099, 623  $\nu(\text{ClO}_4)$  and 526  $\nu(\text{Ru-N})$ . UV–vis ( $\lambda_{\text{max}}$ , nm): 239, 277, 491, 746 (in CH<sub>2</sub>Cl<sub>2</sub>) and 256, 275, 356, 502, 770 (in DMSO). MS (LSI, Scan ES<sup>+</sup>): ( $m/z$ ) 2099 [M]<sup>+</sup>, <sup>1</sup>H-NMR (Acetone-d<sub>6</sub>, TMS,  $\delta$  ppm): 7.78–7.75 (m, 8H, Ar-CH<sub>a,a'</sub>), 7.68–7.63 (m, 8H, Ar-CH<sub>b,b'</sub>), 7.51–7.35 (m, 20H, Ar-CH<sub>1,2,3</sub>), 6.87–6.83 (d, 8H,  $J = 12$ , Ar-CH<sub>c,c'</sub>), 6.38–6.12 (m, 4H, Ar-CH<sub>d,d'</sub>), 4.21–4.19 (d, 4H,  $J = 9$ , NH), 3.73–3.53 (m, 8H, N-<sup>5</sup>CH<sub>2</sub>), 2.50 (s, 8H, N-<sup>6</sup>CH<sub>2</sub>), 2.42 (s, 8H, N-<sup>6</sup>CH<sub>2</sub>), 2.37 (s, 4H, N-CH), 2.26 (s, 8H, Cyc-CH<sub>2</sub>) and 2.01–2.00 (s, 8H,  $J = 3$ , Cyc-CH<sub>2</sub>).

#### [Pd(L)<sub>2</sub>Ru<sub>2</sub>(bpy)<sub>4</sub>](ClO<sub>4</sub>)<sub>2</sub> (**5**)

Yield, 65%; color, dark brown; m.p. = 178 °C.  $\Delta_M = 216/\Omega/\text{cm}^2/\text{mol}$ ,  $\mu_{\text{eff}} = \text{Dia}$ , IR (KBr pellets,  $\nu_{\text{max}}/\text{cm}^{-1}$ ): 3357  $\nu(\text{NH})$ , 3060–3031  $\nu(\text{Ar-H})$ , 2924–2841  $\nu(\text{Aliph-H})$ , 1604  $\nu(\text{C=N})$ , 1362  $\nu(\text{N-O})$ , 1098, 624  $\nu(\text{ClO}_4)$  and 520  $\nu(\text{Ru-N})$ . UV–vis ( $\lambda_{\text{max}}$ , nm, \* = shoulder pik): 234, 240, 296, 316\*, 482\*, 758 (in CH<sub>2</sub>Cl<sub>2</sub>) and 262, 298, 321, 465\*, 758 (in DMSO). MS (LSI, scan ES<sup>+</sup>): ( $m/z$ ) 2057 [M]<sup>+</sup>, <sup>1</sup>H-NMR (acetone-d<sub>6</sub>, TMS,  $\delta$  ppm): 8.20 (d, 8H,  $J = 6$ , Ar-CH<sub>a,a'</sub>), 7.98 (s, 8H, Ar-CH<sub>b,b'</sub>), 7.68 (d, 8H,  $J = 9.3$ , Ar-CH<sub>c,c'</sub>), 7.63 (s, 8H, Ar-CH<sub>d,d'</sub>), 7.60–7.40 (m, 20H, Ar-CH<sub>1,2,3</sub>), 4.41 (s, 4H, NH), 3.66–3.53 (m, 8H, N-<sup>5</sup>CH<sub>2</sub>), 2.95 (s, 8H, N-<sup>6</sup>CH<sub>2</sub>), 2.79 (s, 8H, N-<sup>6</sup>CH<sub>2</sub>), 2.62 (s, 4H, N-CH), 2.16 (s, 8H, Cyc-CH<sub>2</sub>) and 1.98 (s, 8H, Cyc-CH<sub>2</sub>).

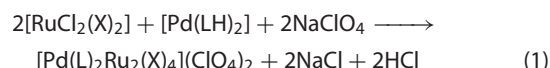
### General procedure for the Suzuki–Miyaura coupling reaction

Catalyst (1.5 mmol% of Pd), aryl halide (1.0 mmol), phenyl boronic acid (1.5 mmol), Cs<sub>2</sub>CO<sub>3</sub> (2 mmol), diethyleneglycol-di-*n*-butylether as internal standard (~30 mg) and DMF (1.5 ml)–H<sub>2</sub>O (1.5 ml) were added to a small Schlenk tube and the mixture was heated at 80 °C in an oil bath. At the end, the mixture was cooled, extracted with Et<sub>2</sub>O, filtered through a pad of silica gel with repeated washings and concentrated. The purity of the compounds was checked by GC and yields are based on aryl halide.

## Results and Discussion

The all complexes are colored, stable to air and light and soluble acetone, dichloromethane, DMF and DMSO. The complexes of the general formula **2** were synthesized by the reactions of ligand (LH<sub>2</sub>) with the respective Pd(CH<sub>3</sub>COO)<sub>2</sub> in a 1 : 2 molar ratio in ethanol; complexes of the general formula **3** were synthesized by the reactions of **2** with the respective excess NaBPh<sub>4</sub> in ethanol; and complexes of the general formula [Pd(L)<sub>2</sub>Ru<sub>2</sub>(X)<sub>4</sub>](ClO<sub>4</sub>)<sub>2</sub> (where X = 1,10 phenanthroline and 2,2'-bipyridine) were synthesized by the reactions of **2** with the respective [RuCl<sub>2</sub>(phen)<sub>2</sub>]:2H<sub>2</sub>O or [RuCl<sub>2</sub>(bpy)<sub>2</sub>]:2H<sub>2</sub>O and NaClO<sub>4</sub> in a 1 : 2 molar ratio in ethanol, as shown in Fig. 2. For the [Pd(L)<sub>2</sub>Ru<sub>2</sub>(X)<sub>4</sub>] complexes,

the reactions of [Pd(LH)<sub>2</sub>] with the system [RuCl<sub>2</sub>(phen)<sub>2</sub>]:2H<sub>2</sub>O or [RuCl<sub>2</sub>(bpy)<sub>2</sub>]:2H<sub>2</sub>O–NaClO<sub>4</sub> were carried out [Eq. (1)].<sup>[19]</sup>



where X = 1,10 phenanthroline and 2,2'-bipyridine. The mass spectra of ligand **1** and **2–5** metal complexes show molecular ion peaks [M]<sup>+</sup> at 465, 1031, 1360, 2099 and 2057 (Fig. 4), respectively, which confirms the proposed structures of the ligand and metal complexes. It is proof that such a hypothesis came from the ESI-MS spectra of compounds. As shown in Fig. 4, the presence of only two peak at  $m/z$  2057.04 and 2057.12 suggested that [Pd(L)<sub>2</sub>Ru<sub>2</sub>(bpy)<sub>4</sub>](ClO<sub>4</sub>)<sub>2</sub> species should be the main species, in the presence of Pd and Ru ions. Magnetic susceptibility measurements provide sufficient data to characterize the structure of the metal complexes. Magnetic moment measurements of all metal complexes were carried out at 25 °C. The results show that mononuclear (**2**) and trinuclear (**3–5**) metal complexes are diamagnetic. The morphology and particle size of the compounds are illustrated by the scanning electron micrography (SEM). Figure 6(a, b) depict the SEM photographs of **2** and **5** complexes. We noted that there is a uniform matrix of the synthesized complexes in the diagram. This leads us to believe that we are dealing with homogeneous phase material. The crystalline shape is observed in the **2** complex with a particle size of 30  $\mu\text{m}$ . The amorphous shape is observed in the **5** complex with a particle size of 100  $\mu\text{m}$ .

### NMR results

The data of the <sup>1</sup>H- and <sup>13</sup>C-NMR spectra obtained for **1–5** metal complexes are given in the Experimental section. The chemical shifts were observed at 9.56 ppm as singlets for C=N–OH groups of oximes in the <sup>1</sup>H NMR spectra of ligand **1**. The chemical shifts which belong to –NH protons were observed at 5.15–5.13 ppm as a doublet for **1**, at 5.82 ppm as a singlet for **2**, at 5.68–5.65 ppm as

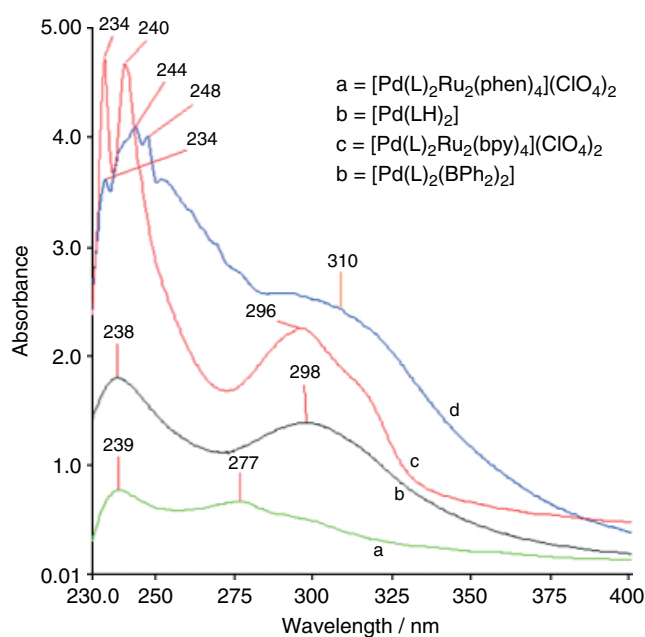


Figure 3. UV absorption spectra of metal complexes in CH<sub>2</sub>Cl<sub>2</sub>.



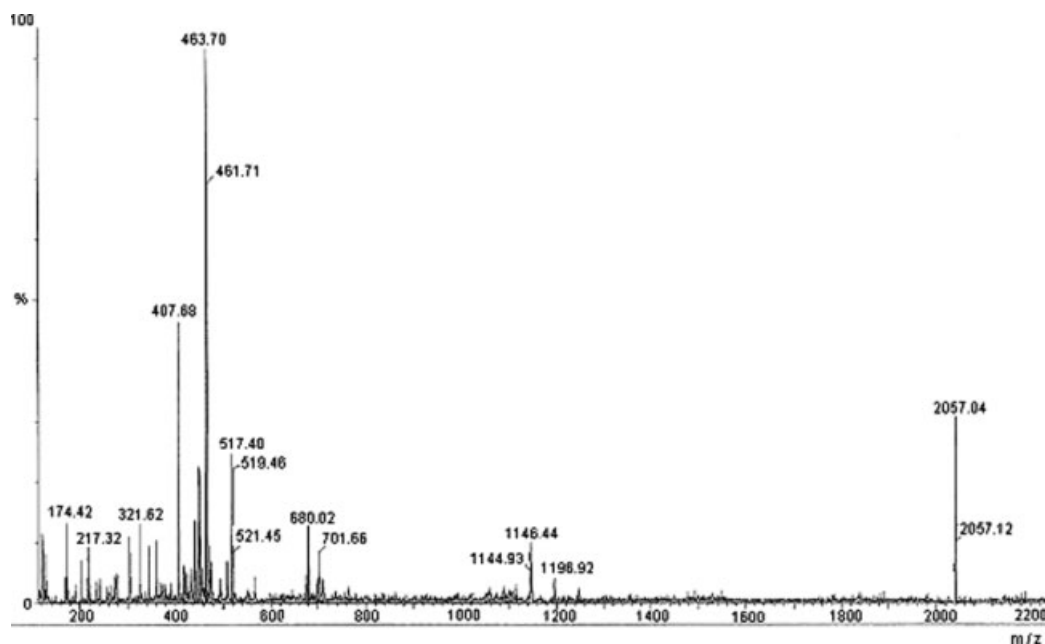


Figure 4. The mass spectrum of **5** metal complex.

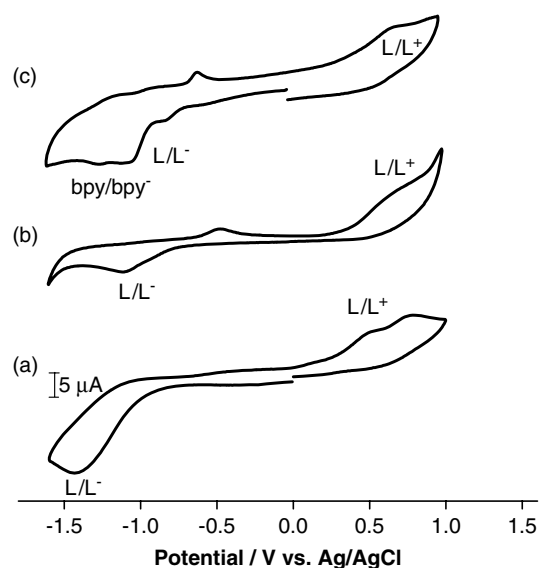


Figure 5. Cyclic voltammograms of **2** (a), **3** (b) and **5** (c) in DMSO solution containing 0.1 M TBAP. Scan rates = 0.100 V/s.

a doublet for **3**, at 4.21–4.19 ppm as doublet for **4** and at 4.41 ppm as singlet for **5**, and disappeared with D<sub>2</sub>O exchange. The <sup>1</sup>H-NMR spectra of the diamagnetic metal complex **2** was characterized by the existence of intra-molecular D<sub>2</sub>O-exchangeable H-bridge (O–H···O) protons, which were observed by a new signals at low field,  $\delta = 16.24$  ppm for **2**. The other protons for **2** were observed at different fields than those of the ligand (in the Experimental section). In the <sup>1</sup>H-NMR spectra of **3**, the D<sub>2</sub>O-exchangeable hydrogen-bridged protons, which were evident in **2**, disappear after the formation of the BPh<sub>2</sub><sup>+</sup>-bridged complex. Indeed, the chemical shifts of the aromatic protons are obtained at 7.33–7.21 ppm as multiplets for **2**, whereas the chemical shifts of the aromatic protons are obtained at 7.77–7.75, 7.65–7.63,

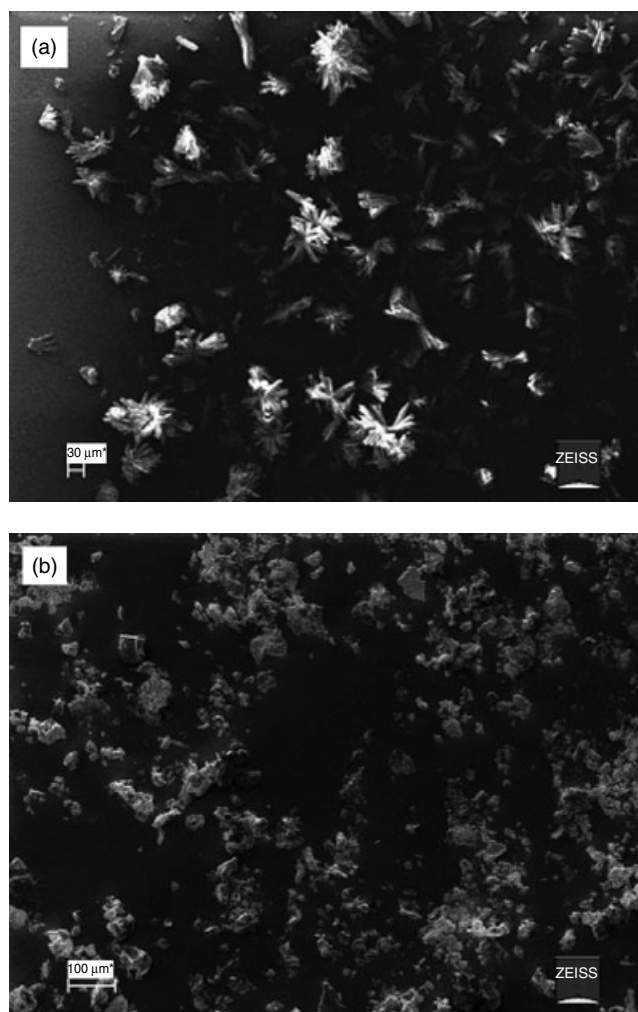


Figure 6. The SEM micrographs of (a) **2** and (b) **5** metal complexes.

7.46–7.11 and 7.03–6.72 ppm as multiplets for (**3**), which proves that the (O–H···O) bridges between the molecules are replaced by BPh<sub>2</sub><sup>+</sup>.<sup>[20]</sup> More detailed information about the structure of ligand **1** is provided by the <sup>13</sup>C-NMR spectrum (in the Experimental section). The chemical shifts for the amide carbon atoms are found at 147.65 ppm for ligand, 152.16 for **2** and 149.62 for **3** complexes.<sup>[20,21]</sup> These equivalent carbon atoms, especially those belonging to hydroxyimino carbon atoms, also confirm the *anti* structure of ligand **1**.<sup>[22]</sup> The chemical shifts of the aromatic carbon atoms were obtained at 127.56, 128.68, 129.43 and 139.01 ppm for **2** complex, whereas the chemical shifts of the aromatic carbons were obtained 127.26, 128.42, 128.91, 138.03, 132.16, 127.68, 127.46 and 126.14 ppm for **3**, which proves that the (O–H···O) bridges between the molecules are replaced by BPh<sub>2</sub><sup>+</sup>. The other chemical shifts (<sup>1</sup>H and <sup>13</sup>C-NMR) belong to BPh<sub>2</sub><sup>+</sup>-capped Pd<sup>II</sup> metal complex **3**, and are very similar to those for the H-bonded Pd<sup>II</sup> metal complex **2**. In the <sup>1</sup>H-NMR spectra of **4** and **5** complexes, the proton Ar–CH<sub>1,2,3</sub> of the phenyl ring is shifted different field compared with that of the free ligand. The <sup>1</sup>H-NMR spectra provide information on the *cis*-coordination of the bpy or phen ligands. As reported previously, each of the pyridine or phenanthroline rings of a bpy or phen ligand are magnetically nonequivalent due to the *cis*-geometry of the complexes.<sup>[17,23]</sup> Therefore, multiplets are observed around at 8.20–6.12 ppm in **4** and **5** complexes and have been assigned to the aromatic protons of **4** and **5** metal complexes.

## IR results

The infrared spectra of ligand **1** with its **2–5** metal complexes were studied in order to characterize their structures. The characteristic infrared spectrum data are given in the Experimental section. In the IR spectrum of the ligand,  $\nu(\text{O–H/N–H})$  stretching vibrations were observed at between 3617 and 3143 cm<sup>–1</sup> for LH<sub>2</sub>. The free *vic*-dioxime ligand showed a strong peak at 1638 cm<sup>–1</sup> for LH<sub>2</sub>, which is characteristic of the azomethine  $\nu(\text{C=N})$  group.<sup>[24]</sup> The  $\nu(\text{C=N})$  stretching vibrations are affected upon complexation and are situated at a frequency significantly different than the free ligands. Coordination of the *vic*-dioxime ligands to the metal center through the four nitrogen atom is expected to reduce the electron density in the azomethine link and lower the  $\nu(\text{C=N})$  absorption frequency. The peak due to  $\nu(\text{C=N})$  was shifted to lower frequencies and appeared between 1610 and 1600 cm<sup>–1</sup>, indicating coordination of the azomethine nitrogen to the Pd metal.<sup>[25]</sup> However, the disappearance of  $\nu(\text{O–H})$  stretching bands in the IR spectrum of free ligand together with the existence of an H-bridge (O–H···O) at 1726 cm<sup>–1</sup> and the shifting of –C=N and –N–O stretches in the IR spectra of the **2** metal complexes provide support for MN<sub>4</sub>-type coordinations in the metal complexes.<sup>[26]</sup> The stretching vibration of (O–H···O) bond at 1726 cm<sup>–1</sup> disappeared upon encapsulation of the H-bonded complex with the appearance of peaks due to the BPh<sub>2</sub><sup>+</sup> contaminant around 1199 and 878 cm<sup>–1</sup> for B–O and B–Ph groups, respectively.<sup>[20]</sup> Perchlorate salts show strong antisymmetric stretching band at between 1099 and 1098 cm<sup>–1</sup> and sharp antisymmetric stretching band at between 624 and 623 cm<sup>–1</sup>, an indication of uncoordinated perchlorate anions.<sup>[27,28]</sup>

## UV–vis spectra

Electronic spectra of ligand **1** and its mononuclear (**2**), trinuclear (**3–5**) metal complexes were recorded in the 200–1100 nm range

in CH<sub>2</sub>Cl<sub>2</sub> and DMSO solutions and their corresponding data are given in the Experimental section. The UV–vis spectra of the ligand and metal complexes in CH<sub>2</sub>Cl<sub>2</sub> showed two-six absorption bands between 230 and 758 nm in CH<sub>2</sub>Cl<sub>2</sub> and two-five absorption bands between 256 and 770 nm in DMSO. The wavelengths of absorption bands appearing in the UV region in both solvents were practically identical. In the electronic spectra of the ligand and its metal complexes, the wide a range bands seem to be due to both the  $\pi \rightarrow \pi^*$ ,  $n \rightarrow \pi^*$  and d–d transitions of C=N and charge-transfer transition arising from  $\pi$  electron interactions between the metal and ligand, which involves either a metal-to-ligand or ligand-to-metal electron transfer.<sup>[29,30]</sup> The absorption bands below 298 nm in CH<sub>2</sub>Cl<sub>2</sub> or DMSO are practically identical and can be attributed to  $\pi \rightarrow \pi^*$  transitions in the benzene ring or azomethine (–C=N) groups. The absorption bands observed within the range 310–316 nm in CH<sub>2</sub>Cl<sub>2</sub> and the range 321–356 nm in DMSO are most probably due to the transition of  $n \rightarrow \pi^*$  of imine group corresponding to the ligand or metal complexes.<sup>[31]</sup> For the mononuclear (**2**) and trinuclear (**3**) complexes, the absorption bands at range 441–437 nm are assigned to M  $\rightarrow$  L charge transfer (MLCT) or L  $\rightarrow$  M charge transfer (LMCT),<sup>[32]</sup> respectively. As expected, the new bands in the range 441–437 nm arising from M  $\rightarrow$  L charge transfer (MLCT) or L  $\rightarrow$  M charge transfer (LMCT) transitions were observed as a result of coordination of palladium metal through azomethine nitrogen. These absorption bands are typical for mononuclear (**2**) and trinuclear (**3**) complexes with a square-planar structure. Complexes **4** and **5** exhibit a shoulder band around 491 with 502 nm and 465 with 482 nm in CH<sub>2</sub>Cl<sub>2</sub> or DMSO, with the absorptivity of the former being higher. These spectra are similar to the other phen or bpy analogs and were assigned to the  $d\pi(\text{Ru}^{\text{II}}) \rightarrow \pi^*$  (phen or bpy) metal-to-ligand charge-transfer (MLCT) transition.<sup>[33]</sup> Examples of UV–vis spectra of the ligand and its metal complexes are presented in Fig. 3 and the Experimental section.

## Solubility and molar conductivity

Ligand **1** is soluble in common organic solvents such as THF, C<sub>2</sub>H<sub>5</sub>OH, CH<sub>2</sub>Cl<sub>2</sub>, and DMSO. Although **2** is soluble in DMSO and DMF and slightly soluble in CH<sub>2</sub>Cl<sub>2</sub>, CHCl<sub>3</sub>, trinuclear metal complexes **3–5** are more soluble than **2** complex, due to the presence of BPh<sub>2</sub><sup>+</sup>, Ru<sub>2</sub>(1, 10-phen)<sub>4</sub>, or Ru<sub>2</sub>(2, 2'-bpy)<sub>4</sub> bridged groups in the oxime moieties. All complexes are stable in the solvents reported in this study at room temperature. With a view to studying the electrolytic nature of the metal complexes, their molar conductivities were measured in DMF at 10<sup>–3</sup> M. The molar conductivity ( $\Lambda_{\text{M}}$ ) values of **2** and **3** metal complexes are in the range 10–30  $\Omega/\text{cm}^2/\text{mol}$  at room temperature,<sup>[18,34]</sup> indicating their almost non-electrolytic nature. Owing to non-free ions in **2** and **3** complexes, the results indicate that these metal complexes have very poor molar conductivity. The molar conductivities ( $\Lambda_{\text{M}}$ ) values of these trinuclear (**4** and **5**) metal complexes were 208–216  $\Omega/\text{cm}^2/\text{mol}$  at room temperature, indicating 1 : 2 electrolytes or three ionic species in solution.<sup>[31b]</sup> The higher values of **4** and **5** complexes than for **2** and **3** complexes indicated the presence of counter ClO<sub>4</sub> ions. Conductivity measurements have frequently been used in structural elucidation of metal chelates within the limits of their solubility. They provide a method for testing the degree of ionization of the complexes; the more molecular ions that a complex liberates in solution (in case of the presence of anions outside the coordination sphere), the higher will be its molar conductivity and vice versa. The molar

conductivity values indicate that the anions may be present outside the coordination sphere or inside or absent.<sup>[34c,d]</sup>

### Crystallography

We attempted to prepare single crystals of ligand **1** with **2–5** metal complexes in different solvents, but we could not prepare convenient single crystals of ligand and all metal complexes. However, the crystalline nature of ligand **1** with **2–5** metal complexes can be readily evidenced from their X-ray powder patterns. The **2** and **3** metal complexes exhibit sharp reflections and all diffractograms are nearly identical, indicating the isostructural nature of the two compounds. Also, the large number of reflections as well as their positions indicates a low crystal symmetry.<sup>[35]</sup> These results show that **2** and **3** metal complexes indicate a crystalline nature, not an amorphous nature, whereas the X-ray powder pattern of **1**, **4** and **5** exhibited only broad humps, not indicating the crystalline nature very well.

### Electrochemistry

The electrochemical properties of **2–5** were investigated using cyclic voltammetric technique in DMSO containing 0.1 M TBAP. Figure 6 represents the cyclic voltammograms (CVs) of the complexes at 0.100 V/s scan rate and their corresponding data are listed in Table 2. As seen from Fig. 5(a), **2** displayed one reduction and one oxidation processes in a DMSO-containing Ag–AgCl electrode system. The reduction and oxidation processes without corresponding anodic or cathodic peaks were irreversible and probably based on the oxime moieties of the complex. The cathodic peak potential of the reduction process was observed at  $E_{pc} = -1.41$  V vs Ag–AgCl while the anodic peak potentials of the oxidation process appeared at  $E_{pa} = 0.51$  and  $0.69$  V as two separated waves because each oxime moieties oxidized at a different potential value. Figure 5(b) indicates the CV of **3**, which displayed a cathodic peak potential at  $E_{pc} = -1.09$  V with a corresponding anodic wave. The value of the cathodic-to-anodic peak separation for the reduction process was calculated as  $0.62$  V in the scan rate of  $0.010$  V/s in DMSO, indicating an irreversible nature of the reduction process. No wave was recorded during cathodic sweep range  $0.0$  to  $-0.70$  V, which confirms that the wave observed at  $E_{pa} = -0.47$  V corresponds to anodic peak of the first reduction process. This irreversible character of the reduction process with the large peak separation is probably caused by low electron transfer on the electrode surface once the complex reduces. The complex also showed one oxidation process with anodic peak potential at  $E_{pa} = 0.69$  V. The process has no a corresponding anodic wave which indicates the irreversible behavior of the oxidation process. These processes are based on the oxime moieties of the complex. The electrochemical behavior of **3** is similar to that of **2** in the same experimental conditions, with the exception that the cathodic peak ( $E_{pc}$ ) potential of **3** shifts toward more positive value compared with that of **2** as a result of the  $BPh_2^+$ -bridged complex formation. The CVs of **4** and **5** exhibited almost the same electrochemical behavior. Figure 5(c) represents the CV of **4** in DMSO containing the Ag–AgCl electrode system at a scan rate of  $0.100$  V/s. The complex displayed two reduction and one oxidation processes. The first reduction and oxidation processes belong to the oxime moieties of the complex and their cathodic and anodic peak potentials appeared at  $E_{pc} = -0.98$  and  $0.69$  V, respectively. The second reduction wave can probably be assigned to a bpy ligand-based reduction

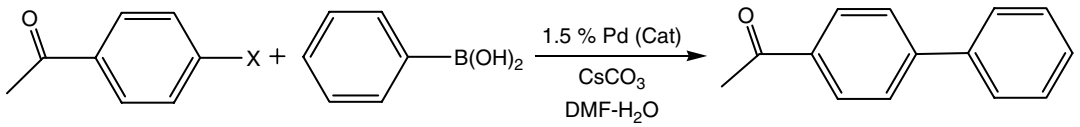
process and its cathodic peak potential ( $E_{pc}$ ) was  $-1.23$  V, which is around that of the complex  $[Ru(bpy)_3]^{2+}$ .<sup>[36]</sup> The oxidation process corresponding to  $Ru^{2+}/Ru^{3+}$  could not be observed in the range of DMSO solution.

### Catalytic tests

The palladium-catalyzed reaction of aryl halides with arylboronic acids (the Suzuki reaction) is the most common method for C–C bond formation.<sup>[11,37]</sup> The reactions are usually carried out homogeneously in the presence of a base under inert atmosphere. The reactivity of the aryl halide component decreases sharply in the order  $X = I > Br > Cl$  and electron withdrawing substituents (R) are required for the chlorides to react.<sup>[11,38]</sup> Also, it is well known that the catalytic activity depends on the aryl ring increasing the reaction rate;<sup>[39]</sup> the electron-donating substituent on the aryl group makes the oxidative addition more difficult and, as a result, electron-poor aryl halides are often referred to as activated, and electron-rich aryl halides as deactivated.<sup>[40]</sup> Herein we initially describe *vic*-oxime-derived metal complexes as air- and water-stable catalysts that are suitable for cross-coupling 4-bromo- and 4-chloroacetophenone with boronic acids in neat water.<sup>[12b]</sup> The different *vic*-oxime derived metal complexes and  $Pd(OAc)_2$  were initially tested *in-situ* as possible candidates to study their catalytic activity on a model coupling reaction between phenylboronic acid with 4-bromo- and 4-chloroacetophenone, summarized in Table 1. In order to find optimum conditions, a series of experiments was performed on 4-bromo- and 4-chloroacetophenone with phenylboronic acid as model compounds. As a base,  $Cs_2CO_3$ <sup>[41]</sup> was the best choice and as a solvent mixture DMF (1.5 ml) and  $H_2O$  (1.5 ml) were found to be better than other solvents. The catalysts were generated *in situ* from  $Pd(OAc)_2$  and ligand **1** or their isolated complexes **2–5** were prepared and compared under the same reaction conditions. From the results in Table 1, this preliminary study has demonstrated that *vic*-dioxime-derived metal complexes are efficient catalysts for a wide range of C–C coupling reactions. However, the bipyridine–Ru complex (**5**) and *in situ* formed catalyst systems [**1** +  $Pd(OAc)_2$ ] were more efficient than the others. Complex **2** had greater selectivity for this coupling reaction. The boron atom made no significant contribution. In conclusion, these novel compounds are active catalysts in the coupling of 4-bromoacetophenone with phenylboronic acid.

### Conclusions

In this study, the new *vic*-dioxime ligand containing the 4-amino-1-benzyl piperidine group, *N,N'*-(4-amino-1-benzyl piperidine)-glyoxime (**1**), and its mononuclear (**2**) and trinuclear (**3–5**) complexes were synthesized and characterized by elemental analyses, FT-IR, UV–vis,  $^1H$ - and  $^{13}C$ -NMR spectra, magnetic susceptibility measurements, molar conductivity, cyclic voltammetry, mass spectra, X-ray powder techniques and their morphology by SEM measurements. This study presents a highly soluble series of the heterotrinnuclear *vic*-dioxime complexes (**3–5**), which were prepared by the coordination of  $BPh_2^+$ ,  $Ru(1,10-phen)_2$ , or  $Ru(2,2'-bpy)_2$  bridged groups into the main palladium oxime moieties. Therefore, the trinuclear (**3–5**) metal complexes studied in the present work will be interesting for many applications in a variety of high technology fields, such as medicine, catalysis, as well as DNA binding and antitumor activity. The comparative electrochemical studies of mono- and trinuclear complexes provide useful information on the electron-transfer reactions of the

**Table 1.** The Suzuki coupling reaction of arylhalides with phenylboronic acid


Entry	1 + Pd(OAc) <sub>2</sub> or complexes 2–5	Time (h)	X	Conversion (%)	Yield (%) <sup>a</sup>
1	1	1	Br	98	96
2	1	2	Br	98	96
3	2	1	Br	93	93
4	2	2	Br	95	95
5	3	1	Br	92	92
6	3	2	Br	95	95
7	4	1	Br	92	92
8	4	2	Br	95	94
9	5	1	Br	97	97
10	5	2	Br	97	97
11	1	2	Cl	44	44
12	1	4	Cl	59	59
13	2	2	Cl	39	39
14	2	4	Cl	44	44
15	3	2	Cl	26	25
16	3	4	Cl	29	29
17	4	2	Cl	30	30
18	4	4	Cl	33	33
19	5	2	Cl	43	42
20	5	4	Cl	45	44
21	– <sup>b</sup>	2	Cl	12	12
22	1	2	Cl	28 <sup>c</sup>	28

*Reaction conditions:* 1.0 mmol of aryl halide; 1.5 mmol of phenylboronic acid; 2.0 mmol Cs<sub>2</sub>CO<sub>3</sub>; %1.5 Pd (cat.) was used; DMF, 1.5 ml–H<sub>2</sub>O 1.5 ml; temperature, 80 °C.  
<sup>a</sup> GC yield using diethyleneglycol-di-*n*-butylether as internal standard.  
<sup>b</sup> 1.5% Pd(OAc)<sub>2</sub> was used as catalyst.  
<sup>c</sup> 1.0% Pd (Cat.).

**Table 2.** Voltammetric data for the complexes in DMSO-TBAP

Complexes	bpy/bpy <sup>–</sup> or phen/phen <sup>–</sup> , E <sub>pc</sub> <sup>a</sup> (V)	L/L <sup>–</sup> , E <sub>pc</sub> <sup>a</sup> (V)	L/L <sup>+</sup> , E <sub>pa</sub> <sup>a</sup> (V)
[Pd(LH) <sub>2</sub> ]		–1.41	0.51, 0.69
[Pd(L) <sub>2</sub> (BPh <sub>2</sub> ) <sub>2</sub> ]		–1.09	0.69
[Pd(L) <sub>2</sub> Ru <sub>2</sub> (phen) <sub>4</sub> ](ClO <sub>4</sub> ) <sub>2</sub>	–1.23	–0.98	0.61
[Pd(L) <sub>2</sub> Ru <sub>2</sub> (bpy) <sub>4</sub> ](ClO <sub>4</sub> ) <sub>2</sub>	–1.23	–0.98	0.69

<sup>a</sup> Cathodic peak potential for reduction, anodic peak potential for oxidation for irreversible processes.

electro-reduced or electro-oxidized species in nonaqueous solution. The catalytic results show that the bipyridine–Ru complex (5) and *in situ*-formed catalyst systems [1 + Pd(OAc)<sub>2</sub>] are more efficient than the others.

### Acknowledgments

This work was supported, in part, by the Research Fund of Harran University (Sanliurfa, Turkey).

### References

- [1] M. Kurtoglu, M. M. Dagdelen, S. Toroglu, *Trans. Met. Chem.* **2006**, *31*, 382; b) R. B. Lauffer, *Chem. Rev.* **1987**, *87*, 190; c) G. T. Muise, X. Li, D. R. Powell, *Inorg. Chim. Acta* **2004**, *357*, 1134.
- [2] A. Chakravorty, *Coord. Chem. Rev.* **1974**, *13*, 1.
- [3] J. P. Leonardo, D. P. Novotnik, R. D. Neirincx, *J. Nucl. Med.* **1986**, *27*, 1819.
- [4] J. R. Dilworth, S. J. Parrott, *Chem. Soc. Rev.* **1998**, *27*, 43.
- [5] I. H. Hall, K. F. Bastow, A. E. Warren, C. R. Barnes, G. M. Bouet, *Appl. Organometal. Chem.* **1999**, *13*, 819.
- [6] E. Lukevics, R. Abele, M. Fleisher, J. Popelis, E. Abale, *J. Mol. Catal. A Chem.* **2003**, *198*, 89.
- [7] D. Sellman, J. Utz, F. W. Heinemann, *Inorg. Chem.* **1999**, *38*, 459.
- [8] M. C. M. Laranleira, R. A. Marusak, A. G. Lappin, *Inorg. Chim. Acta* **2000**, *186*, 300.
- [9] K. Ohta, R. Hisaghi, M. I. Kejima, I. Yamamoto, N. Kobayashi, *J. Mater. Chem.* **1998**, *8*, 1979.
- [10] S. Kumar, R. Singh, H. Singh, *J. Chem. Soc. Perkin Trans.* **1992**, *1*, 3049.
- [11] N. Miyaruna, A. Suzuki, *Chem. Rev.* **1995**, *95*, 2457; b) A. J. Suzuki, *J. Organomet. Chem.* **1999**, *576*, 147; c) S. P. Stanforth, *Tetrahedron* **1998**, *54*, 263; d) G. T. Crisp, *Chem. Soc. Rev.* **1998**, *27*, 427; e) N. J. Whitcombe, K. K. Hii, S. E. Gibson, *Tetrahedron* **2001**, *57*, 7449; f) N. T. S. Phan, M. V. D. Sluys, C. W. Jones, *Adv. Synth. Catal.* **2006**, *348*, 609; g) F. Alonso, I. P. Beletskaya, M. Yus, *Tetrahedron* **2008**, *64*, 3047.
- [12] S. Haber, H. J. Kleiner, (Hoescht AG), DE 19527118 [*Chem. Abstr.* **1997**, *126*, 185894]; b) L. Botella, C. Najera, *Angew. Chem. Int. Edn* **2002**, *41*, 179.



- [13] M. L. Kantouri, C. D. Papadopolous, M. Quiros, A. G. Hatzidimitriou, *Polyhedron* **2006**, 26, 1292; b) S. Srinivasam, J. Annaraj, P. R. Athappan, *J. Inorg. Biochem.* **2005**, 99, 876.
- [14] F. Karapcin, S. Ilcan, Y. Caglar, M. Caglar, B. Dede, Y. Sahin, *J. Organomet. Chem.* **2007**, 692, 2473.
- [15] B. P. Sullivan, J. A. Baumann, T. J. Meyer, D. J. Salmon, H. Lehmann, A. Ludi, *J. Am. Chem. Soc.* **1977**, 99, 7368; b) W. H. Fung, W. Y. Fu, C. M. Che, *J. Org. Chem.* **1998**, 63, 7715; c) T. H. Ghaddar, E. W. Castner, S. S. Isied, *J. Am. Chem. Soc.* **2000**, 122, 1233.
- [16] B. J. Sullivan, D. J. Salmon, T. J. Meyer, *Inorg. Chem.* **1978**, 17, 3334.
- [17] R. Llanguri, J. J. Morris, W. C. Stanley, E. T. Bell-Loncella, M. Turner, W. J. Bayko, C. A. Bessel, *Inorg. Chim. Acta* **2001**, 315, 53.
- [18] A. Kilic, E. Tas, I. Yilmaz, *J. Chem. Sci.* (in press).
- [19] B. R. Manzano, F. A. Jalon, G. Espino, A. Guerrero, R. M. Claramunt, C. Escolastico, J. Elguero, M. A. Heras, *Polyhedron* **2007**, 26(15), 4373; b) P. J. Steel, E. C. Constable, *J. Chem. Soc. Dalton Trans.* **1990**, 1389.
- [20] M. Durmus, V. Ahsen, D. Luneau, J. Pecaut, *Inorg. Chim. Acta* **2004**, 357, 588.
- [21] H. O. Kalinowski, S. Berger, S. Braun, <sup>13</sup>C-NMR-Spektroskopie. Georg Thieme: New York, **1984**.
- [22] Y. Gok, H. Kantekin, H. Alp, M. Ozdemir, *Z. Anorg. Allg. Chem.* **1995**, 621, 1237.
- [23] E. Bell-Loncella, C. A. Bessel, *Inorg. Chim. Acta* **2000**, 303, 199; b) F. E. Lytle, L. M. Petrosky, L. R. Carlson, *Anal. Chim. Acta* **1971**, 57, 239.
- [24] K. N. Kumar, R. Ramesh, *Polyhedron* **2005**, 24, 1885; b) A. Kilic, E. Tas, B. Gumgum, I. Yilmaz, *Trans. Met. Chem.* **2006**, 31, 645.
- [25] S. A. Ali, A. A. Soliman, M. M. Aboaly, R. M. Ramadan, *J. Coord. Chem.* **2002**, 55, 1161.
- [26] M. Kandaz, A. Koca, A. R. Ozkaya, *Polyhedron* **2004**, 23, 1987; b) E. Tas, M. Aslanoglu, A. Kilic, Z. Kara, *J. Coord. Chem.* **2006**, 59(8), 861.
- [27] M. R. Rosenthal, *T. Chem. Edu.* **1973**, 50, 331.
- [28] F. Karapcin, B. Dede, Y. Caglar, D. Hur, S. Ilcan, M. Caglar, Y. Sahin, *Optics Comm.* **2007**, 272, 131.
- [29] L. Sacconi, M. Ciampolini, F. Maffio, F. P. Cavasino, *J. Am. Chem. Soc.* **1962**, 84, 3245; b) A. Kilic, E. Tas, B. Deveci, I. Yilmaz, *Polyhedron* **2007**, 26, 4009.
- [30] R. L. Carlin, *Transition Metal Chemistry*, vol. 1. Marcel Dekker: New York, **1965**.
- [31] C. Fraser, B. Bosnich, *Inorg. Chem.* **1994**, 33, 338; b) S. Ilhan, H. Temel, I. Yilmaz, A. Kilic, *Trans. Met. Chem.* **2007**, 32, 344.
- [32] A. B. P. Lever, *Inorganic Electronic Spectroscopy*. Elsevier: Amsterdam, **1984**; b) E. Tas, V. T. Kasumov, O. Sahin, M. Ozdemir, *Trans. Met. Chem.* **2002**, 27, 442.
- [33] R. Hage, J. H. Van Diemen, G. Ehrlich, J. G. Haasnoot, D. J. Stufkens, T. L. Snoeck, J. G. Vos, J. Reedjick, *Inorg. Chem.* **1990**, 29, 988; b) M. Murali, M. Palaniandavar, *Polyhedron* **2007**, 26(14), 3980.
- [34] R. L. Dutta, *Inorganic Chemistry*, Part II, 2nd edn. The New Book Stall: Calcutta, **1981**, p. 386; b) A. Kilic, E. Tas, B. Gumgum, and I. Yilmaz, *Polish J. Chem.* **2006**, 80, 1967; c) M. S. Refat, S. A. El-Korashy, D. N. Kumar, A. S. Ahmad, *Spectrochim. Acta A* (doi:10.1016/j.saa.2007.10.005); d) M. S. Refat, *J. Mol. Struct.* **2007**, 742(1–3), 24.
- [35] B. R. Srinivasan, N. S. Dhuri, C. Nathar, and W. Bensch, *Trans. Met. Chem.* **2007**, 32, 64; b) A. Kilic, and E. Tas, *Synth. React. Inorg. Met.-Org. Chem. and Nano-Met. Chem.* **2007**, 37, 583.
- [36] X. Liu, J. Liu, K. Jin, X. Yang, Q. Peng, L. Sun, *Tetrahedron* **2005**, 61, 5655.
- [37] B. Gumgum, N. Biricik, F. Durap, I. Ozdemir, N. Gurbuz, W. H. Ang, P. J. Dyson, *Appl. Organometal. Chem.* **2007**, 21, 711.
- [38] A. F. Littke, G. F. Fu, *Angew. Chem. Int. Edn Eng.* **2002**, 41, 4176; b) R. B. Bedford, S. L. Hazewood, M. E. Limmeat, *Chem. Commun.* **2002**, 2610.
- [39] I. P. Beletskaya, A. V. Cheprakov, *Chem. Rev.* **2000**, 100, 3009.
- [40] N. J. Whitcombe, K. K. Hii (Mimi), S. E. Gibson, *Tetrahedron* **2001**, 57, 7449; b) M. Keles, Z. Aydin, O. Serindag, *J. Organomet. Chem.* **2007**, 692, 1951.
- [41] C. Zhang, J. Huang, M. L. Trudell, S. P. Nolan, *J. Org. Chem.* **1999**, 64, 3804.